

29 Mar 2001, 4:00 pm - 6:00 pm

Comparison and Modeling of Sand Behavior Under Cyclic Direct Simple Shear And Cyclic Triaxial Testing

J.-F. Vanden Berghe
Université Catholiques de Louvain, Belgium

A. Holeyman
Université Catholiques de Louvain, Belgium

R. Dyvik
Norwegian Geotechnical Institute, Norway

Follow this and additional works at: <https://scholarsmine.mst.edu/icrageesd>



Part of the [Geotechnical Engineering Commons](#)

Recommended Citation

Vanden Berghe, J.-F.; Holeyman, A.; and Dyvik, R., "Comparison and Modeling of Sand Behavior Under Cyclic Direct Simple Shear And Cyclic Triaxial Testing" (2001). *International Conferences on Recent Advances in Geotechnical Earthquake Engineering and Soil Dynamics*. 34.
<https://scholarsmine.mst.edu/icrageesd/04icrageesd/session01/34>



This work is licensed under a [Creative Commons Attribution-Noncommercial-No Derivative Works 4.0 License](#).

This Article - Conference proceedings is brought to you for free and open access by Scholars' Mine. It has been accepted for inclusion in International Conferences on Recent Advances in Geotechnical Earthquake Engineering and Soil Dynamics by an authorized administrator of Scholars' Mine. This work is protected by U. S. Copyright Law. Unauthorized use including reproduction for redistribution requires the permission of the copyright holder. For more information, please contact scholarsmine@mst.edu.



COMPARISON AND MODELING OF SAND BEHAVIOR UNDER CYCLIC DIRECT SIMPLE SHEAR AND CYCLIC TRIAXIAL TESTING.

Vanden Berghe, J-F.

Université catholique de Louvain
Louvain-La-Neuve, Belgium.

Holeyman, A.

Université catholique de Louvain
Louvain-La-Neuve, Belgium

Dyvik, R.

Norwegian Geotechnical Institute
Oslo, Norway

ABSTRACT

Constant volume cyclic shear (DSS) tests were performed on Brusselian sand using the new NGI simple shear apparatus and a special control system for cyclic strain controlled testing. Test results are compared with those from cyclic triaxial (TXS) tests. The tests investigated the degradation of the cyclic shear modulus for different relative densities (from 60% to 90%), different consolidation pressures (from 50kPa to 200kPa) and different shear strain amplitudes (from 0.1% to 9%). The comparison of the soil specimen behavior in the two different test types shows that soil degradation is mainly function of (1) the dilative or contractive behavior of the soil and of (2) the extreme state reached during the previous cycles. The test results show that there exists a unique relationship between the secant shear modulus of a given cycle and the energy dissipated during that cycle. A model is presented that predicts the hysteresis loops induced on a dilative soil during a cyclic strain controlled direct simple shear test.

SCOPE OF THE RESEARCH

The research focuses on the degradation of sand under large cyclic strain. That phenomenon is characterized by means of cyclic strain controlled triaxial tests and direct simple shear tests. The influence of shear strain amplitude, γ_a , (from 0.1% to 9%), relative density, D_r , (from 60% to 90%) and consolidation pressure, σ_3' or σ_v , (from 50kPa to 200kPa) is investigated.

The sand used in this investigation is Brusselian sand of tertiary stage. It is characterized by a mean diameter, d_{50} , of 0.18mm and an uniformity coefficient, C_u , of 2.2. Its maximum and minimum void ratios are 1.18 and 0.52, respectively.

The present article presents similitudes between the cyclic triaxial (TXS) tests and the cyclic direct simple shear (DSS) tests: the influence of the dilative/contractive behavior, the shape of the γ (shear strain) – τ (shear stress) curve and the shape of the hysteresis loops. The article also presents a method to calculate hysteresis loops for a dilative soil using Masing rules (Masing, 1926).

EXPERIMENTAL PROCEDURES AND TEST RESULTS

Cyclic Triaxial (TXS) Test

Test Procedure. Cyclic TXS tests were performed on compacted Brusselian sand specimens at the Université Catholique de Louvain (Belgium). The specimens height was 200mm and their diameter was 100mm.

Each specimen is prepared by the method of moist tamping in 10 layers using the undercompaction method (Ladd, 1978). The procedure takes into account that, when a sand is compacted in layers, the compaction of each succeeding layer can further densify the sand below it. Therefore, each layer is compacted to a lower density than the final desired value by predicting the amount of required undercompaction. This undercompaction amount in each layer linearly varies from the bottom to the top of the specimen.

After compaction, the air in the specimen is replaced by CO_2 which facilitates the saturation of the specimen. After saturation, the specimen is consolidated under an isotropic stress field, σ_3' .

After the soil reaches equilibrium, it is sheared by a cyclic variation of the axial strain. The test is undrained while the pore pressure is continuously measured. The shear strain amplitudes, γ_a , used in this investigation cover the shear strains from 0.1% to 6%. The frequency of this cyclic displacement is 0.005Hz. During the test, the lateral pressure is regulated to maintain constant the total

mean stress p (i.e. $\Delta\sigma_3 = -\Delta\sigma_1/2$).

Test Results. Figure 1 shows a typical hysteresis curve γ (shear strain) – τ (shear stress) for a cyclic triaxial test. Because the mode of deformation of the specimen is not the same in extension and in compression, the curves are not symmetric. The curves pass through two fixed points (F & F' on Figure 1). In each case, these fixed points roughly correspond to zero shear stress and always occur where the specimen exhibits a contractive behavior. The shear strain corresponding to the fixed points is more or less 2/3 of the strain amplitude, γ_a .

Figure 2 shows the evolution as a function time of the shear stress compared with the pore pressure, u . The pore pressure has a double frequency: during each cycle, two periods of dilation ($\Delta u > 0$) and two of contraction ($\Delta u < 0$) are observed. The end of each dilation phase corresponds to the maximum shear strain whereas the end of each contraction phase corresponds with the inflexion point of the shear stress curve of the hysteresis curve (points I_1, I_2, I_3, I_4 & I_5 on Figure 2). That means that more energy has to be expended to shear the specimen when it has a dilative behavior than a contractive behavior. The explanation could be that it is more difficult to dislodge a grain out of the soil matrix than push it back into the hole where it was.

Except for the first cycle, the moment where the pore pressure exceeds the maximum pore pressure observed during the previous cycles roughly corresponds to zero shear stress (points M_1, M_2, M_3 & M_4 on Figure 2). In the previous paragraph, it was seen that the fixed points observed on the hysteresis curves (F & F') corresponds also to zero shear stress. Therefore, the fixed point and the point where the pore pressure is equal to the maximum pore pressure observed previously may be assumed to occur simultaneously. However, a detailed analysis shows that the fixed point usually slightly precedes the point where the pore pressure is

equal to the maximum pore pressure observed during the previous cycles.

Generally, two parameters are used to represent the different cycles: the secant shear modulus, G_{s_n} , and the energy dissipated during each cycle, W_n . The secant shear modulus, G_{s_n} [MPa], is defined as the slope measured between the two extreme points tips of the hysteresis loop (Equation 1). The energy dissipated during the cycle, W_n [MJ/m³], is proportional to the area bounded by the hysteresis curve.

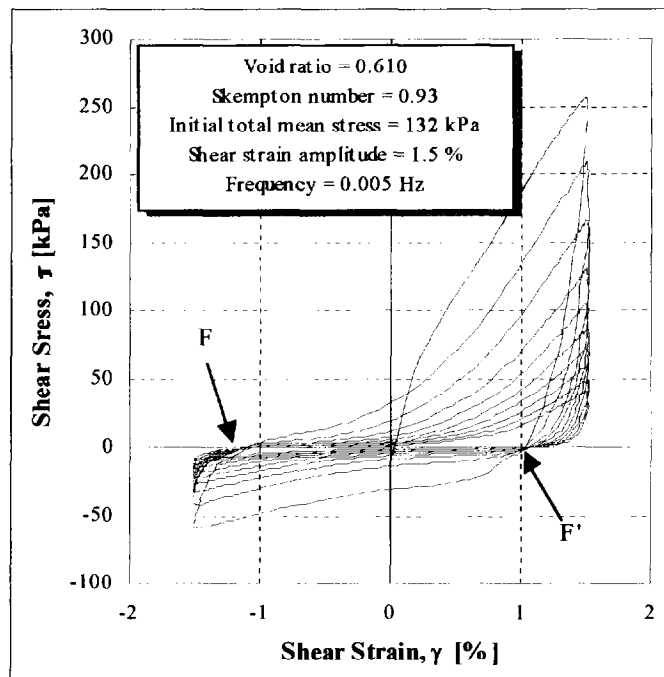


Fig. 1: Hysteresis loops during an undrained cyclic TXS test

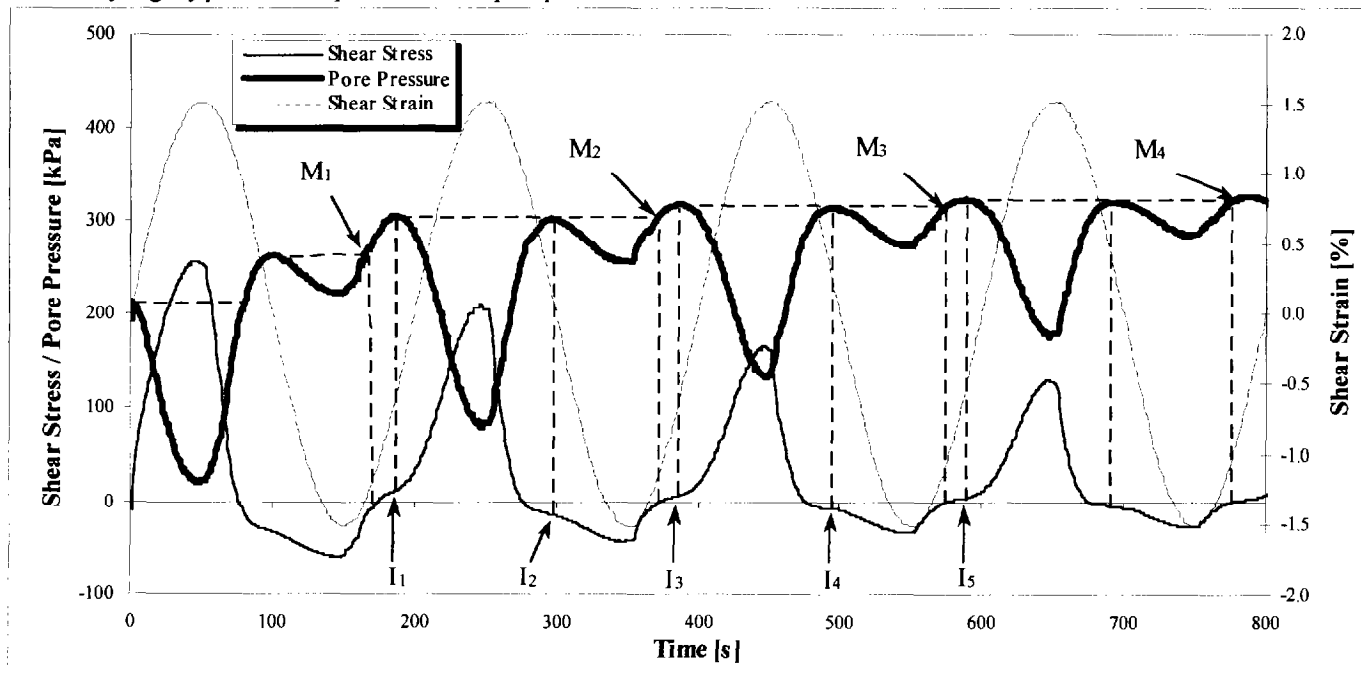


Fig. 2: Comparison of shear stress, shear strain and pore pressure during an undrained cyclic TXS test.

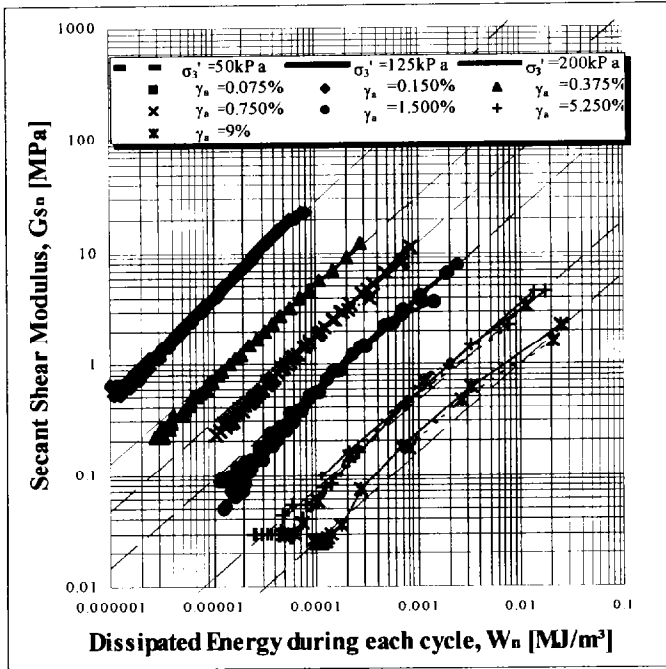


Fig. 3: $G_{sn} - W_n$ relationship for undrained different cyclic TXS tests investigating different strain amplitudes γ_a and consolidation stresses σ_3' ($Dr=85\%$).

$$G_{S_n} = \frac{\Delta \tau_{\max}}{2 \cdot \gamma_a / 100} \quad (1)$$

Figure 3 presents the relationship between the secant shear modulus, G_{sn} , and the energy dissipated during each cycle, W_n , for the different strain amplitudes investigated. There exists an exponential relationship between those two parameters that can be represented by Equation 2.

$$G_{S_n} = a \cdot W_n^b \quad (2)$$

The value of the exponent b is nearly constant for all the tests performed and is equal to 0.8 where G_{sn} is expressed in MPa and W_n in MJ/m^3 . The parameter a seems to be only dependent on the strain amplitude γ_a and is independent of the relative densities and the consolidation stress investigated. The value of parameter a is

drawn in Figure 4 as a function of the shear strain amplitude for different relative densities and consolidation stresses. The followed exponential equation fits rather well to the experimental results:

$$a = 2000 \cdot \gamma_a^{-1.8} \quad (3)$$

Taking into account Equation 3, Equation 2 can be rewritten as

$$G_{S_n} = 2000 \cdot \frac{W_n^{0.8}}{\gamma_a^{1.8}}, \text{ or} \quad (4)$$

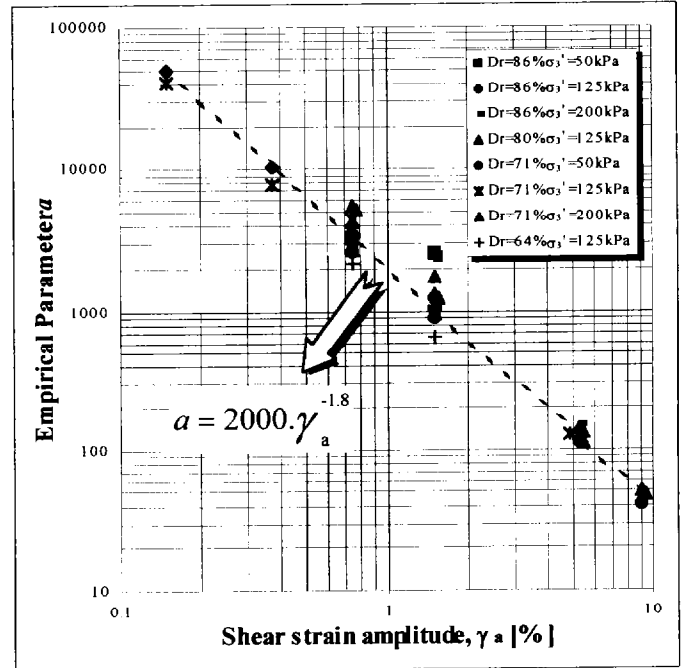


Fig. 4: Evolution of the parameter a of Equation 2 as a function of the shear strain amplitude γ_a , the relative density Dr and the consolidation stress σ_3' for undrained cyclic TXS tests.

$$\Delta \tau_{\max} = 4000 \cdot \left(\frac{W_n}{\gamma_a} \right)^{0.8} \quad (5)$$

G_{sn} in MPa, W_n in MJ/m^3 , $\Delta \tau_{\max}$ in MPa and γ_a in %

This relationship indicates that a unique relationship exists between the extremum points of a hysteresis curve and its shape.

Cyclic Direct Simple Shear (DSS) Test

Test Procedure. The new NGI direct simple shear apparatus (Fig. 5) whose control system has been modified to allow cyclic strain controlled simple shear testing, is used for this research. This device was designed by the Norwegian Geotechnical Institute.

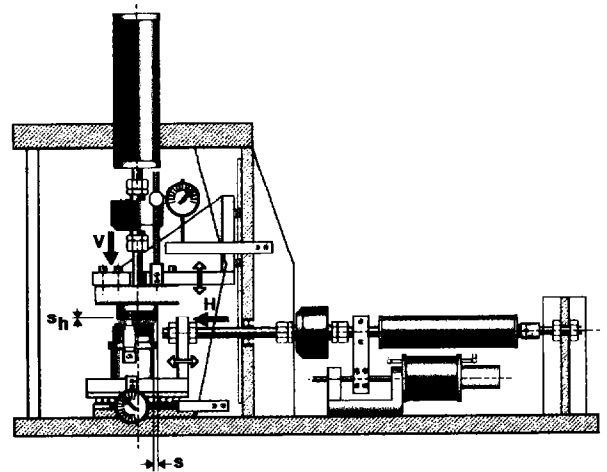


Fig. 5: New NGI simple shear apparatus.

This apparatus allows the shearing of a soil specimen in a such way that uniform shear strain results throughout the sample. This is accomplished by translating the base of the specimen horizontally relative to the fixed specimen top. The specimen is confined within a wire reinforced rubber membrane that, while permitting specimen vertical and shear displacements, does not permit specimen radial strain. The membrane used is reinforced by iron-nickel wire with a diameter of 0.2mm. The wire is wound at 30 turns per centimeter of membrane height (0.3mm center to center spacing).

This apparatus allows one to control either strains or stresses in both horizontal and vertical directions during consolidation and during shear. This is applied enforced by two electrical motors (linear actuators).

The initial specimen height is 16mm and its diameter is 66.7mm (i.e. a surface area of 35cm²). The specimen is prepared by the method of moist tamping in one lift. The specimen is tamped directly in the reinforced membrane in two different operations. The first operation consists in locally tamping a given weight of sand to obtain the same compaction near the membrane as in the middle of the specimen. After placing the top cap on the specimen, the second operation consists in tamping the specimen on the entire surface until the specimen height corresponding to the desired relative density is reached.

After preparation, the specimen is loaded by applying progressively a vertical constant motor speed of 0.03mm/min. After reaching the desired axial stress σ_v , a flow of CO₂ is percolated through the specimen. The specimen is then saturated by flushing water. The pressure of the pore water is maintained equal to atmospheric pressure during the consolidation and the cyclic test.

It is important to note that in the simple shear test, the consolidation of the specimen is anisotropic. The specimen is consolidated under K_0 conditions.

After consolidation, the soil specimen is cyclicly sheared in the horizontal direction. The shear strain amplitudes γ_a used in this investigation range from 0.25% to 9%. The frequency of this cyclic deformation is 0.0005Hz.

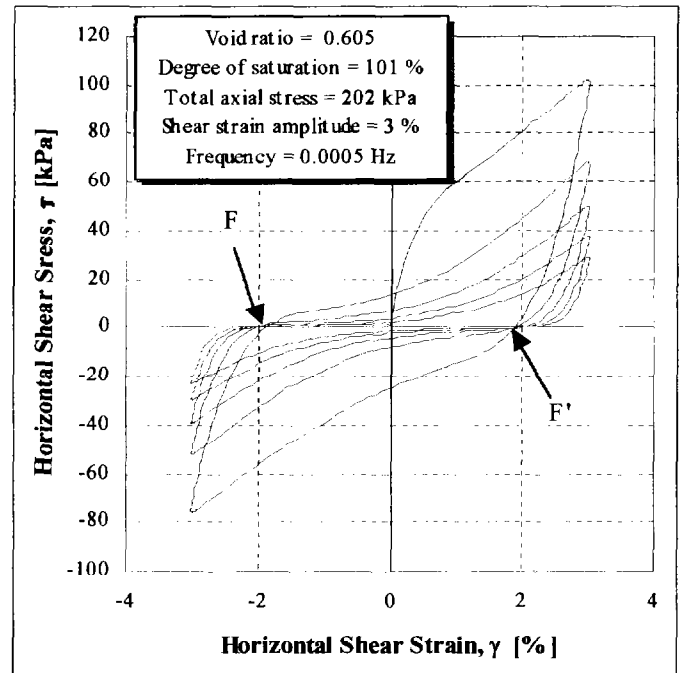


Fig. 6: Hysteresis loops during a cyclic constant volume DSS test.

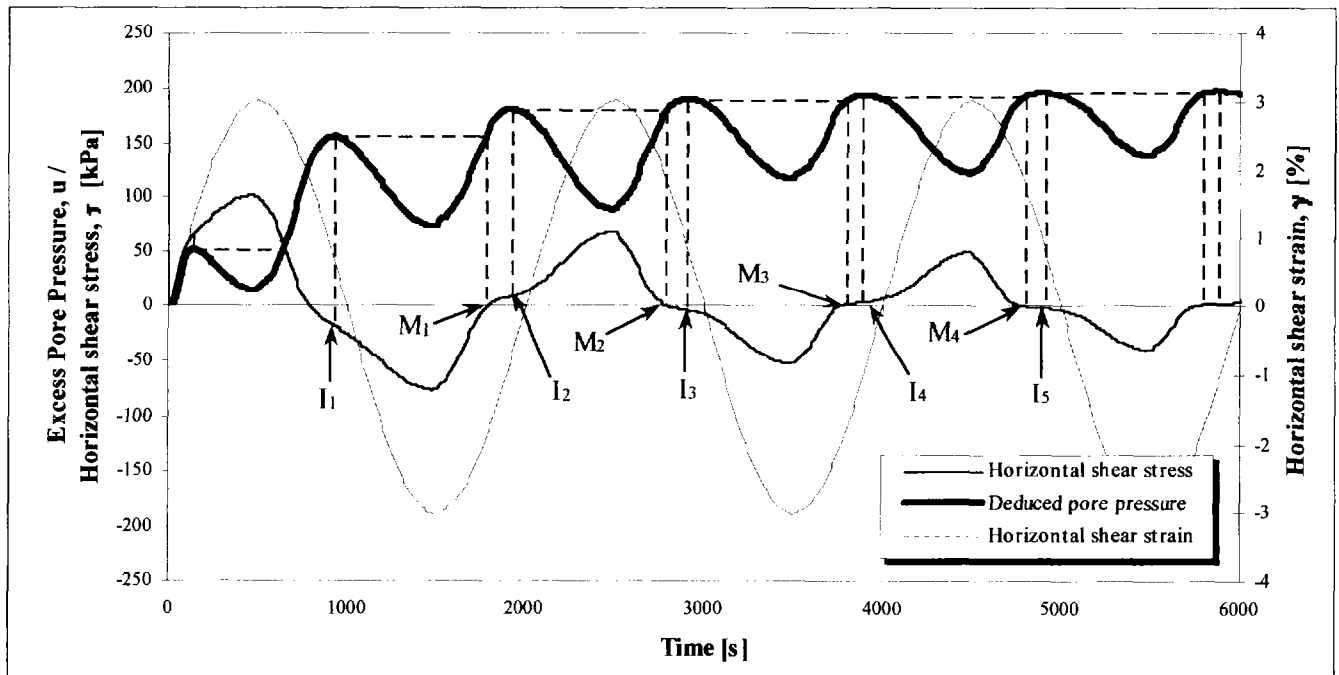


Fig. 7: Comparison of horizontal shear stress, horizontal shear strain and pore pressure during an undrained cyclic DSS test.

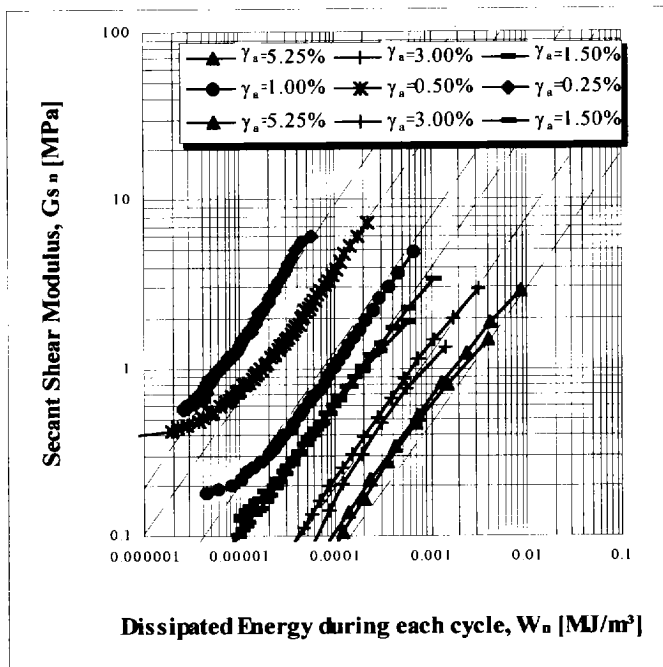


Fig. 8: $G_{sn} - W_n$ relationship for different undrained cyclic DSS tests investigating different strain amplitudes, γ_a ($D_r=85\%$; $\sigma_v=200\text{kPa}$)

All the tests are constant volume tests. Since the wire-reinforced membrane prevents radial specimen strain, the specimen volume is held constant by maintaining a constant specimen height. This is accomplished by changing the vertical stress applied on the specimen. This change in the vertical stress is assumed to be equivalent to the excess pore pressure buildup in an undrained test (Dyvik and al., 1987). Therefore, the total vertical stress is assumed to remain constant during the test. In theory, it is not necessary to saturate the specimen during a DSS test because there is no real pore pressure generation in the specimen. However, poor saturation can modify soil resistance as a result of capillary effects. In the following, the constant volume DSS tests are called undrained DSS test.

DSS Test Results. Figure 6 shows the hysteresis curves observed during a cyclic DSS test. The shape of the curves is similar to that of the shear stress curve observed during the cyclic TXS tests, except that in the DSS test the curve is symmetric. The pore pressure surmized from DSS test is also similar to that measured during the triaxial test (Fig. 7):

- The pore pressure has a double frequency (two periods of dilation and contraction per cycle). The end of each dilation phases corresponds with the maximum shear strain whereas the end of each contraction phase corresponds with the inflexion point of the shear stress curve (points I_1, I_2, I_3, I_4 & I_5 on Figure 7).
- The shear stress where the pore pressure is equal to the maximum pore pressure observed during the previous cycles corresponds to the zero shear stress (points M_1, M_2, M_3 & M_4 on Figure 7).

The hysteresis curves also present two fixed points (F & F' on Figure 6). In each case, the fixed point roughly correspond to the maximum pore pressure observed during the previous cycles.

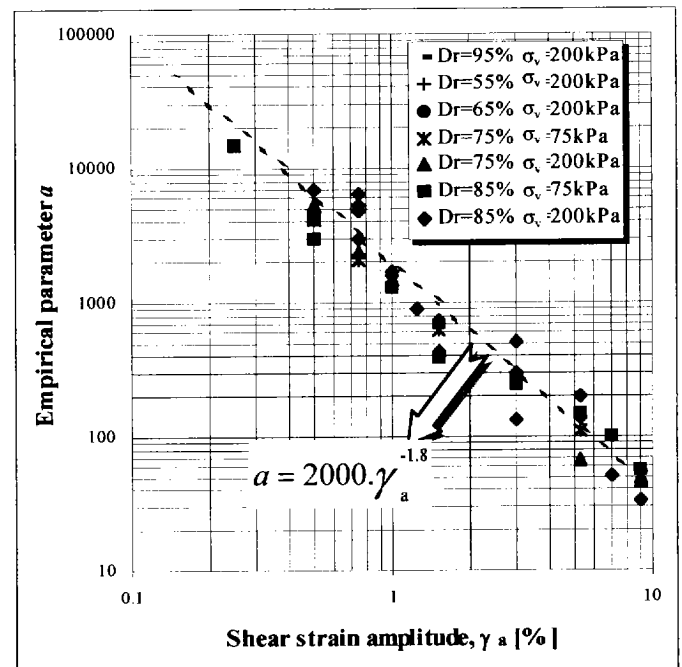


Fig. 9: Evolution of the parameter a of Equation 2 as a function of the shear strain amplitude, γ_a , the relative density, D_r , and the vertical consolidation stress, σ_v' , for undrained cyclic DSS tests.

As initially noted for the triaxial tests, the analysis of the cyclic DSS test results indicates (Fig. 8) that an exponential relationship exists between the secant shear modulus and the energy dissipated during the corresponding cycle. Equation 5 defined for the TXS tests also applies to DSS test results, as portrayed in Figure 9.

MODELING OF A DILATIVE SOIL DURING CYCLIC DSS TESTING

A method frequently used in earthquake engineering to construct hysteresis loops consecutive to cyclic motion is based on the Masing rules (Masing, 1926). This method uses the curve obtained from monotonic loading, called a backbone curve (curve OA on Figure 10). The unloading branch of the loop (curve ADB) is obtained by two-fold stretching of the backbone curve about B, translating its origin O to the point of stress reversal A. In the same way, the reloading curve (curve BCA) is obtained enlarging the backbone curve by a factor of two about A, shifting its origin O to the point of stress reversal B.

Traditionally, the backbone curve used follows a hyperbolic model (Kondner, 1963). Unfortunately, that model has a concave shape (as represented on Figure 10) and is unable to represent the S-shape of the hysteresis curve observed with the Brusselian sand (Fig. 1 and Fig. 6). Therefore, the backbone curve has to be extended to introduce an inflexion point and a convex part when the soil has a dilative behavior. The new backbone curve proposed in this article (Equation 6) is divided in two terms:

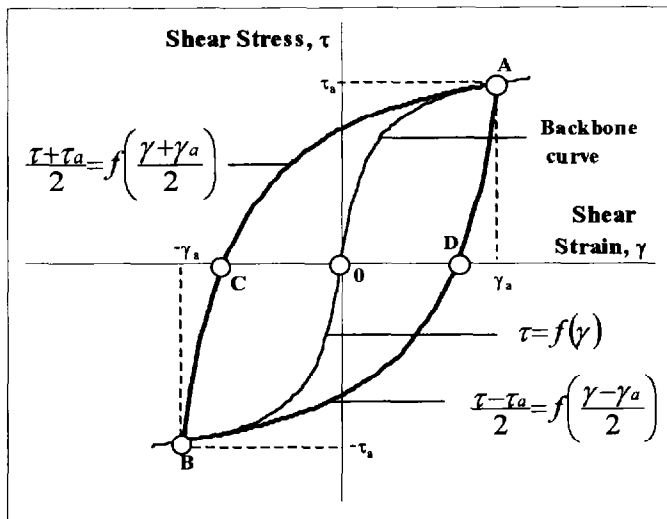


Fig. 10: Hysteresis loops constructed using the Masing rules and the Kondner model.

$$\tau = \frac{G_{\max} \cdot \gamma}{1 + \frac{G_{\max} \cdot \gamma}{\tau_c}} + \frac{A \cdot \gamma^2 + B \cdot \gamma}{C + \gamma} \quad (6)$$

The first term is active during the beginning of the shearing and represents the strain-stress curve during the contractive behavior (concave part of the curve). This term tends rapidly to a constant value. It is function of three parameters: G_{\max} , γ and τ_c . G_{\max} is equal to the slope of the curve at the origin. τ_c (c for contraction) is the maximum soil resistance induced during the contractive phase. The second term has a convex shape. During a monotonic loading, it is observed that, before reaching failure of the specimen, the

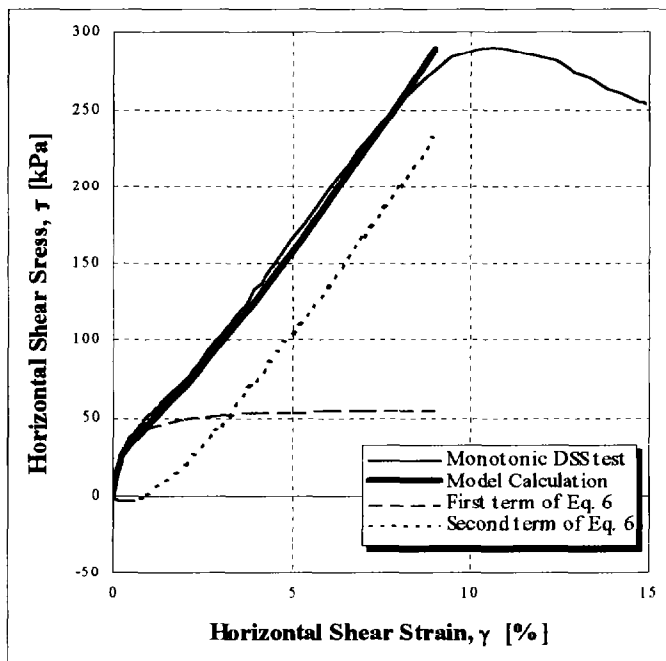


Fig. 11: Comparison of the backbone curve and its different terms with a monotonic undrained DSS test ($\sigma_v=200\text{kPa}$, $D_r=85\%$).

shear stress-shear strain curve follows an oblique straight line. Therefore, the expression of the second term of Equation 6 tends towards an oblique tangent (characterized with slope A and a value at the origin B, see Figure 11). The third parameter of the second term C defines the curvature of the curve.

This equation does not take into account that the specimen tends towards a limit state during the shearing. The shear resistance increases indefinitely. Therefore, the range where the equation is applicable is limited. Figure 11 compares the proposed backbone curve with a monotonic DSS test. The values of the 5 parameters of Equation 6 are listed in Table 1.

Table 1. Values of the model parameters

	Units	Monotonic DSS test	Cyclic DSS Test			
			Cycle 2	Cycle 5	Cycle 10	Cycle 20
G_{\max}	MPa	20	20	20	20	20
τ_c	kPa	51	46	28	17	8
A	kPa	3500	3500	3500	3500	3500
B	kPa	-30	-30	-30	-30	-30
C	-	0.02	0.0089	0.0091	0.0120	0.0289

The new backbone curve (Equation 6) combined with the Masing rules is used to calculate the hysteresis loops measured during a cyclic undrained DSS test. The model calculates closed loops for each cycle based on degradation of the cycle. It does not take into account the increasing degradation within a cycle. The Figures 12 to 15 compare the results of the model with the experiment. Table 1 shows the value of the different parameters of the backbone curve (Equation 6). The parameters G_{\max} , A and B are constant for all cycles and are identical to those deduced from the monotonic test. The degradation is taken into account in the parameters τ_c and C (Fig 16). Using the empirical relationship between the secant shear modulus G_{s_n} and the energy dissipated during the cycle W_n (Equation 4), the parameter C can be evaluated as a function of the parameter τ_c . Therefore, this model is able to predict the degradation of a cyclic test as a function of one parameter: τ_c . As presented on Figure 16, the evolution of the parameter τ_c can be described using a semi-logarithmic relationship (Equation 7) that is function of two parameters $\tau_{c \text{ monotonic}}$ and α .

$$\tau_c = \tau_{c \text{ monotonic}} \cdot (1 - \text{LOG}_{10}(N^{\alpha})) \quad (7)$$

$\tau_{c \text{ monotonic}}$ is the value of τ_c deduced from the monotonic test whereas α is the parameter that describes the soil degradation. The number of cycles needed to reach the complete degradation N_{deg} can be deduced from this parameter.

$$N_{\text{deg}} = 10^{\frac{1}{\alpha}} \quad (8)$$

For the example presented above, the value of N_{deg} is 36.5. That value corresponds perfectly to the number of cycles resulting in a secant shear modulus, G_{s_n} , of 0 and an excess pore pressure equal to the consolidation effective stress.

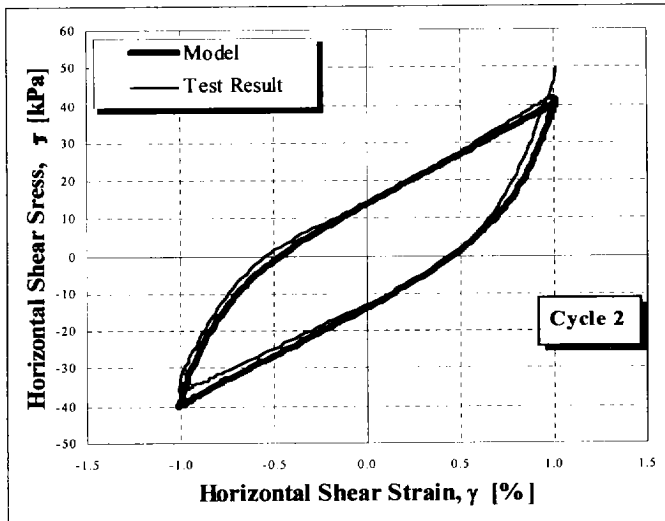


Fig. 12: Comparison of the 2nd cycle of an undrained DSS test ($\sigma_v=200\text{kPa}$, $D_r=85\%$) with the proposed model.

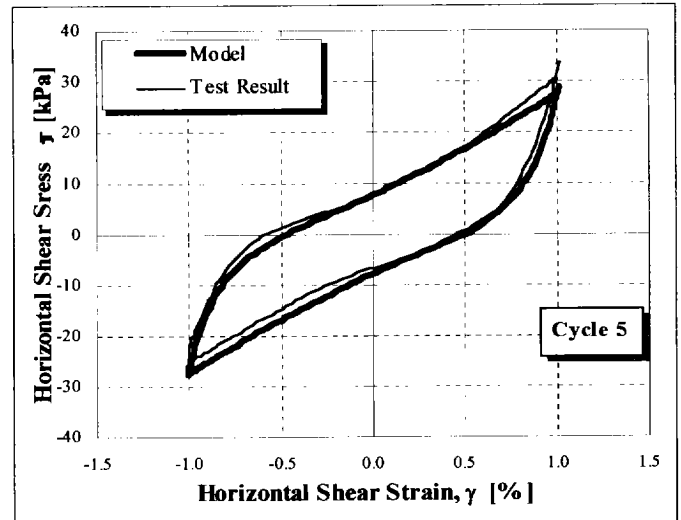


Fig. 13: Comparison of the 5th cycle of an undrained DSS test ($\sigma_v=200\text{kPa}$, $D_r=85\%$) with the proposed model.

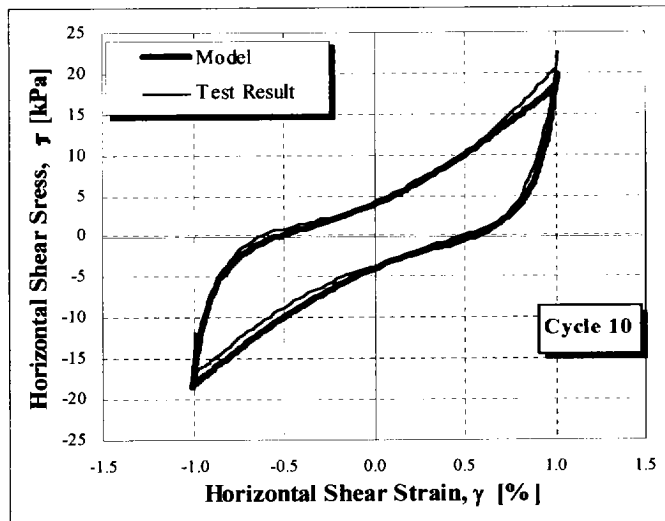


Fig. 14: Comparison of the 10th cycle of an undrained DSS test ($\sigma_v=200\text{kPa}$, $D_r=85\%$) with the proposed model.

In summary (Fig. 17), the model presented herein is able to predict the hysteresis loops of a dilative soil induced during a cyclic DSS test based on:

- The results on a monotonic test performed with the same relative densities and consolidation stress
- A degradation law that calculates the number of cycles need to reach the complete degradation of the soil as a function of the soil type, the relative densities, the consolidation stress and the strain amplitude
- A relationship between the secant shear modulus, $G_{s,n}$, and the energy dissipated during the corresponding cycle, W_n , as a function of the soil type and the strain amplitude.

CONCLUSIONS

The comparison of the behavior of the soil specimen under DSS and TXS testing shows that soil degradation is mainly function of (1) the dilative or contractive behavior of the soil and of (2) the

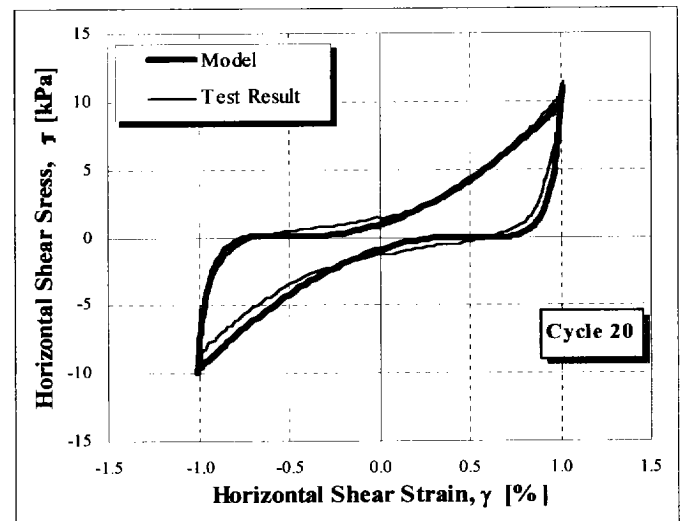


Figure 15: Comparison of the 20th cycle of an undrained DSS test ($\sigma_v=200\text{kPa}$, $D_r=85\%$) with the proposed model.

maximum state reached during the previous cycles. The test results show that a unique relationship exists between the secant shear modulus of a cycle, $G_{s,n}$, and the energy dissipated during the corresponding cycle, W_n . This relationship is only function of the soil type and the strain amplitude of the tests. The shape of the hysteresis is not arbitrary but is function of the extremum points of the loop.

A new expression of the backbone curve was introduced to take into account the S-shape of the shear stress-shear strain curve during a DSS test. The equation was defined with two terms: the first is active during the contractive phase of the shearing whereas the second describes the dilative behavior of the soil. The hysteresis loops were calculated using Masing rules. From the 5 parameters describing the loops (see Equation 6), 3 of them (A, B and G_{max}) are calculated from the results of a monotonic test. The relationship between the secant shear modulus of a cycle, $G_{s,n}$, and the energy dissipated during the corresponding cycle, W_n , can be used to eliminate one other parameter. Therefore, the model

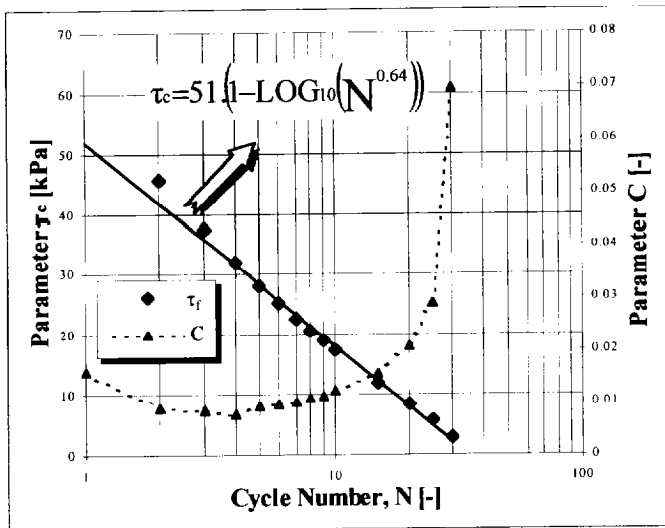


Fig. 16: Evolution of the parameter τ_c and C as a function of cycle number N

presented is able to calculate the cyclic response of Brusselian sand under cyclic DSS in function of one parameter (τ_c). The evolution of this parameter as a function of the cycle number is semi logarithmic. That relationship is characterized with parameters deduced from a monotonic test ($\tau_{c \text{ monotonic}}$) and from a degradation law (N_{deg}).

The future development of the research will try to improve the form of the backbone curve to be able to describe asymmetrical loops as observed during a cyclic triaxial test.

ACKNOWLEDGMENTS

The authors want to thank the European Commission (Marie Curie Research Training Grant) and the Fonds National de la Recherche Scientifique (FNRS) who funded this research. All our thanks go to the Norwegian Geotechnical Institute for the use of the direct simple shear apparatus in their laboratory. Finally, we thank the personnel of the NGI laboratory and of the Civil Engineering Laboratory (LGC) of the UCL, in particular Mr. E. Bouchonville, for their help in the conduct of the tests.

REFERENCES

Bjerrum, L. and Landva A. 1966. Direct Simple Shear tests on a Norwegian quick clay. *Geotechnique*, Vol 16, No. 1, pp.1-20

Dyvik, R., Berre T., Lacasse S. and Raadim B. 1987. Comparison of trully undrained and constant volume direct simple shear tests. *Geotechnique*. vol. 37, No. 1, pp.3-10

Kondner, R. L. 1963. Hyperbolic Stress -Strain Response: Cohesive Soils. *Journal of Soil Mechanics and Foundations Division, ASCE*, vol. 89, No. SN1, pp.115-143

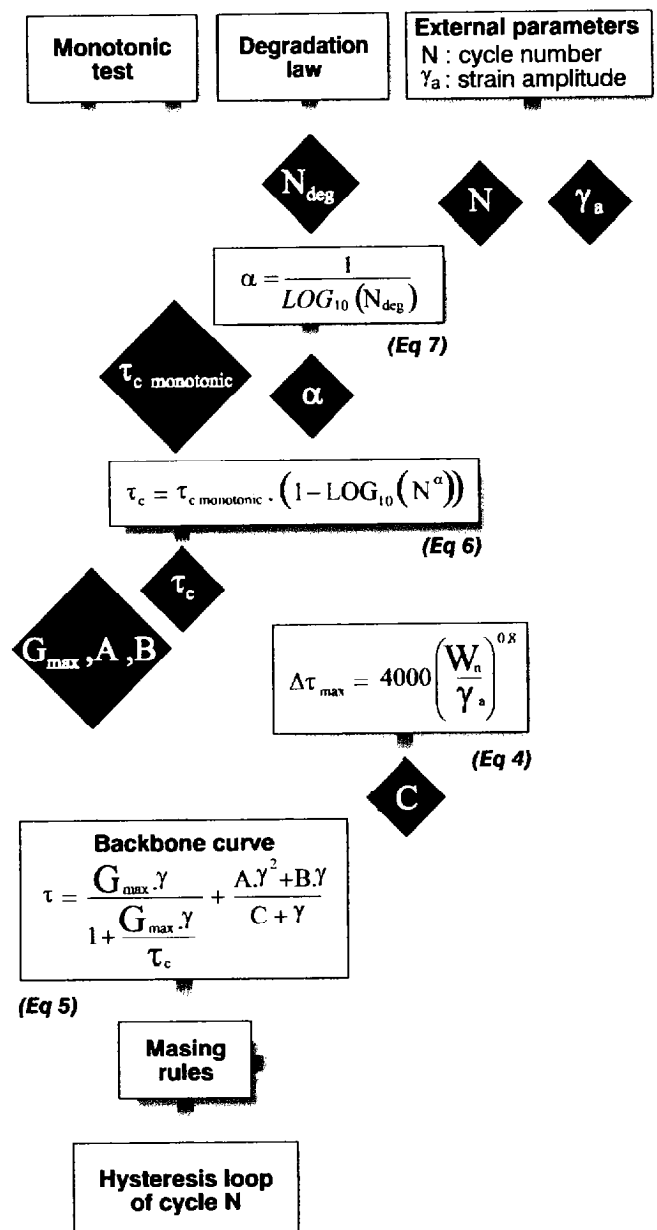


Fig. 17: Proposed model description.

Ladd R.S. 1978. Preparing Test Specimens Using Undercompaction. *Geotechnical Testing Journal, GTJODJ*, vol. 1, No 1, march 1978, pp.16-23

Masing, G. 1926. Eigenspannungen und Verfeistigung beim Messing, *Proceeding of second International Congress of Applied Mechanics*, pp.332-335.